In Vivo Demonstration of Red Cell–Endothelial Interaction, Sickling and Altered Microvascular Response to Oxygen in the Sickle Transgenic Mouse

Dhananjaya K. Kaul,* Mary E. Fabry,* Frank Costantini,‡ Edward M. Rubin,§ and Ronald L. Nagel*

**Division of Hematology, Albert Einstein College of Medicine and Montefiore Medical Center, New York 10461; ‡Department of Genetics and Development, Columbia University, New York 10027; and §Cell and Molecular Biology Division, Lawrence Berkeley Laboratory, Berkeley, California 94720*

Abstract

Intravascular sickling, red cell–endothelium interaction, and altered microvascular responses have been suggested to contribute to the pathophysiology of human sickle cell disease, but have never been demonstrated under in vivo flow. To address this issue, we have examined a transgenic mouse line, $\alpha^{H}\beta^{S}\beta^{S\text{-Antilles}}[\beta^{MDD}]$ which has a combined high (78%) expression of β^{S} and $\beta^{S\text{-Antilles}}$ globins.

In vivo microcirculatory studies using the cremaster muscle preparation showed adhesion of red cells, restricted to postcapillary venules, in transgenic mice but not in control mice. Electron microscopy revealed distinct contacts between the red cell membrane and the endothelium surface. Some red cells exhibiting sickling were regularly observed in the venular flow. Infusion of transgenic mouse red cells into the ex vivo mesocecum vasculature also showed adhesion of mouse red cells exclusively in venules.

Under resting conditions (pO_2, 15–20 mmHg), there were no differences in the cremaster microvascular diameters of control and transgenic mice; however, transgenic mice showed a drastic reduction in microvascular red cell velocities (Vrbc) with maximal Vrbc decrease (> 60%) occurring in venules, the sites of red cell adhesion and sickling. Local, transient hyperoxia (pO_2, 150 mmHg) resulted in striking differences between control and transgenic mice. In controls, oxygen caused a 69% arteriolar constriction, accompanied by 75% reduction in Vrbc. In contrast, in transgenic mice, hyperoxia resulted in only 8% decrease in the arteriolar diameter and in 68% increase in Vrbc; the latter is probably due to an improved flow behavior of red cells as a consequence of unsickling.

In summary, the high expression of human sickle hemoglobin in the mouse results not only in intravascular sickling but also red cell–endothelium interaction. The altered microvascular response to oxygen could be secondary to blood rheological changes, although possible intrinsic differences in the endothelial cell/vascular smooth muscle function in the transgenic mouse may also contribute. These sickle transgenic mice could serve as a useful model to investigate vasoocclusive mechanisms, as well as to test potential therapies. (*J. Clin. Invest.* 1995. 96:2845–2853.) Key words: microcirculation • red cell adhesion • sickling • oxygen tension • vessel diameter

Introduction

Sickle cell anemia (SS)[1] is the consequence of a single amino acid substitution (β6Glut→Val) in the hemoglobin (Hb) molecule, resulting in the polymerization of HbS molecules and sickling of red cells under deoxy conditions. The effect of this single-point mutation is not limited to the ability of red cells to sickle, but results in pleiotropic abnormalities such as hemolysis, red cell heterogeneity, increased red cell adhesivity, vascular endothelial injury, and multiple organ damage (1). Although HbS polymerization is central to the pathophysiology of vasoocclusion, the role of multiple factors (both primary and secondary) in the initiation of vasoocclusion has not been investigated under in vivo flow conditions. Among these factors, adhesion of SS cells to the vascular endothelium has been suggested to play an important role in vasoocclusion. Increased adhesion of SS cells was first demonstrated by Hebbel and coworkers (2, 3) using endothelial cell cultures, and later confirmed by others in both static and flow systems (4–6). Finally, adhesion was demonstrated in an ex vivo microcirculatory bed (7–9) and found to be restricted to venules. Increased adhesion of SS cells in microcirculation could lead to an increased red cell capillary transit time and intravascular sickling.

We have previously used a *trans*-species ex vivo microvasculature to understand vasoocclusive behavior of human SS cells (7–9). Although these ex vivo studies have advanced our understanding of adhesive and obstructive behavior of heterogenous SS red cell classes, as well as of microvascular sites (venules) of adhesion (7–9), the results of these acute *trans*-species infusion experiments need to be verified in vivo, preferably in an intraspecies model. Transgenic mouse models, in particular, provide with an opportunity to investigate potential vasoocclusive mechanisms and to resolve the question if mouse red cells containing human sickle hemoglobin could adhere. Although several transgenic mouse lines expressing human sickle hemoglobin have been well characterized (10–15), there has been no intravital study to address these issues.

This work was presented in part at the annual meeting of the American Society of Hematology, Nashville, TN, 2–5 December 1994, and has appeared in abstract form (1994. *Blood*. 81:220*a*).

Address correspondence to Dhananjaya K. Kaul, Ph.D., Department of Medicine, U-917, Albert Einstein College of Medicine, 1300 Morris Park Avenue, Bronx, NY 10461.

Received for publication 14 June 1995 and accepted in revised form 28 August 1995.

J. Clin. Invest.

0021-9738/95/12/2845/09 $2.00
Volume 96, December 1995, 2845–2853

1. *Abbreviations used in this paper:* Hb, hemoglobin; Hct, hematocrit; MCHC, mean corpuscular hemoglobin concentration; PRU, peripheral resistance unit; Q, estimated volumetric flow rate; SS, sickle cell anemia; TEM, transmission electron microscopy; Tpf, pressure-flow recovery time; Vrbc, red cell velocity.

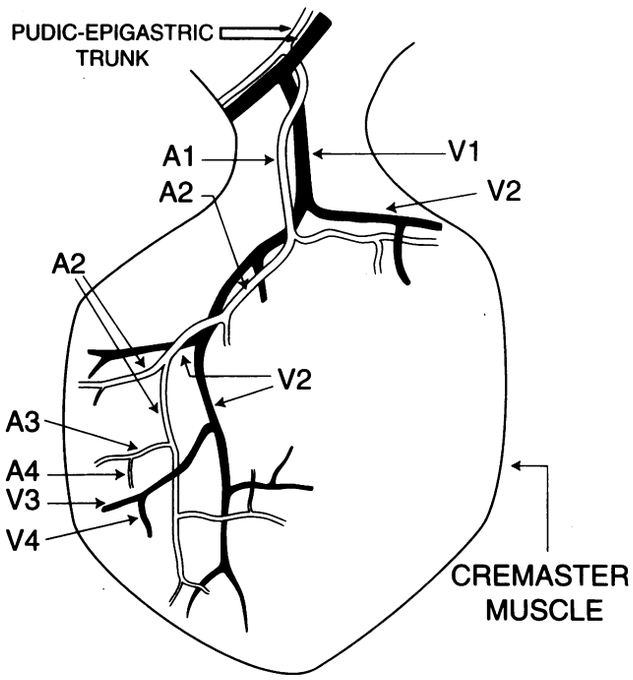

Figure 1. Schematic drawing of the branching patterns of arterioles (*A1–A4*) and venules (*V1–V4*) in the cremaster muscle of C57 BL/6J mouse.

To this end, we have studied a transgenic mouse line expressing human α-, β^S- and $\beta^{S\text{-Antilles}}$-globins on the mouse homozygous β major deletional (β^{MDD}) background (16). These mice were produced by breeding $\alpha^H\beta^S[\beta^{MDD}]$ mice (14) into a line expressing human $\beta^{S\text{-Antilles}}$ on the mouse homozygous β major deletional background (12). $\beta^{S\text{-Antilles}}$ contains, in addition to the HbS mutation at β6, a second mutation at β23 (Val→Ile). $\beta^{S\text{-Antilles}}$ has low oxygen affinity and decreased solubility under deoxygenated conditions, resulting in a more severe form of sickle cell anemia. In $\alpha^H\beta^S\beta^{S\text{-Antilles}}[\beta^{MDD}]$ mice, the combined expression of human β^S and $\beta^{S\text{-Antilles}}$ was 78%. This transgenic mouse line showed a more severe phenotype than either parent, a distinct heterogeneity of red cells (increased reticulocyte counts and presence of dense cells), a decreased delay time of polymerization, more severe organ damage, and a reduced life expectancy (16). Now, we demonstrate that $\alpha^H\beta^S\beta^{S\text{-Antilles}}[\beta^{MDD}]$ mouse red cells are not only more prone to sickling, but also to adhesion under in vivo dynamic flow conditions. Furthermore, adhesion and sickling have significant consequences for red cell velocity, wall shear rates, and the flow throughout the microvasculature. These transgenic mice also show a markedly altered response of the arteriolar diameter and flow to transient hyperoxia.

Methods

Transgenic mice. Transgenic mice expressing human α, β^S and $\beta^{S\text{-Antilles}}$ on the mouse β major deletional background (β^{MDD}) ($\alpha^H\beta^S\beta^{S\text{-Antilles}}[\beta^{MDD}]$) were produced by breeding $\alpha^H\beta^S[\beta^{MDD}]$ mice into a line expressing α^H and $\beta^{S\text{-Antilles}}$ (12) on the mouse β major deletional background, as described (16). Mice were bled from the tail and blood samples analyzed for reticulocytes by using New Methylene Blue or by staining with thiazole orange and performing FACS® analysis (Lysys II, Becton-Dickinson, San Jose, CA). The globin composition was determined by HPLC, as described (16) and revealed the following: human α 58.2% of all α globin, β^S 42.2% and $\beta^{S\text{-Antilles}}$ 35.9% for all β globin (16). Mean corpuscular hemoglobin concentration (MCHC), MCH, and mean corpuscular volume were determined as described (16).

Microcirculatory studies in the cremaster muscle preparation. Male C57 BL/6J control and $\alpha^H\beta^S\beta^{S\text{-Antilles}}[\beta^{MDD}]$ mice weighing ~ 22–28 grams were used. In vivo microcirculatory observations were made in the cremaster muscle microvasculature, which is an easily accessible vasculature for intravital observations. Mice were anesthetized i.p. with 10% urethane and 2% α-chloralose in saline (6 ml/kg). The animals were tracheotomized and the left carotid artery cannulated to monitor systemic arterial pressure. The open cremaster muscle was prepared according to the method of Baez (17). The surface of the open cremaster muscle was suffused with a bicarbonate Ringer's solution of the following millimolar composition: NaCl 135.0, KCl 5.0, $NaHCO_3$ 27.0, $MgCl_2$ 0.64 and glucose 11.6. pH was adjusted to 7.35–7.4 by continuous bubbling with 94.6% N_2 and 5.6% CO_2. The osmolarity of the solution, as measured by a Microosmette (Precision Systems, Inc., Sudsbury, MA) was 320 mOsm which is similar to that reported for the mouse plasma (18). The cremaster muscle preparation was allowed to stabilize for 30 min before the initiation of the experiment. The temperature of the suffusion solution (flow rate, 5–6 ml/min) bathing the cremaster was maintained at 34.5–35°C and monitored by a telethermometer (YSI Inc., Yellowsprings, OH) during the entire experiment. Oxygen tension of the suffusion solution bathing the tissue was determined using a microoxygen electrode (model MI-730; Microelectrodes Inc., Bedford, NH). Microscopic observations were carried out using microscope (model BH-2; Olympus Corp., Lake Success, NY) equipped with a television camera (5000 Series; Cohu, Inc., San Diego, CA) and a Sony U-matic video recorder (model VO5800; Sony Corp., Teaneck, NJ).

The C57 mouse cremaster (Fig. 1) is typically supplied by a single feed arteriole (diameter, 60–75 μm), which originates from the pudic–epigastric trunk. The feed arteriole usually bifurcates at a short distance (0.7–1.0 cm) into daughter vessels; the latter also bifurcate downstream into identical branches (diameters, 40–55 μm). The daughter branches spread out to supply different areas of the cremaster. We have termed the parent vessel as A1 arteriole and the daughter branches as A2 arterioles. Third order arterioles (A3) arise at right-angle from A2 arterioles and give rise to A4 arterioles in a similar fashion. The feed arteriole (A1), because of its upstream location, could not always be transillumi-

Table I. Hematological Parameters in Control and $\alpha^H\beta^S\beta^{S\text{-Antilles}}$ [β^{MDD}] Mice

Mouse	Hct	MCHC	MCV	MCH	Reticulocytes
	%	*grams/dl*	μm^3	*pg*	%
Control (n = 3–5)	49.0±3.1	33.3±0.9	45.4±0.9	14.5±1.0	4.9±0.6
β^S + $\beta^{S\text{-Antilles}}$ (n = 7)	44.7±4.2*	36.7±1.1‡	43.8±1.5	14.7±0.5	9.4±2.3‡

MCV, mean corpuscular volume; MCH, mean corpuscular hemoglobin. Values are mean±SD. * $P < 0.05$ and ‡ $P < 0.01$ as compared with control.

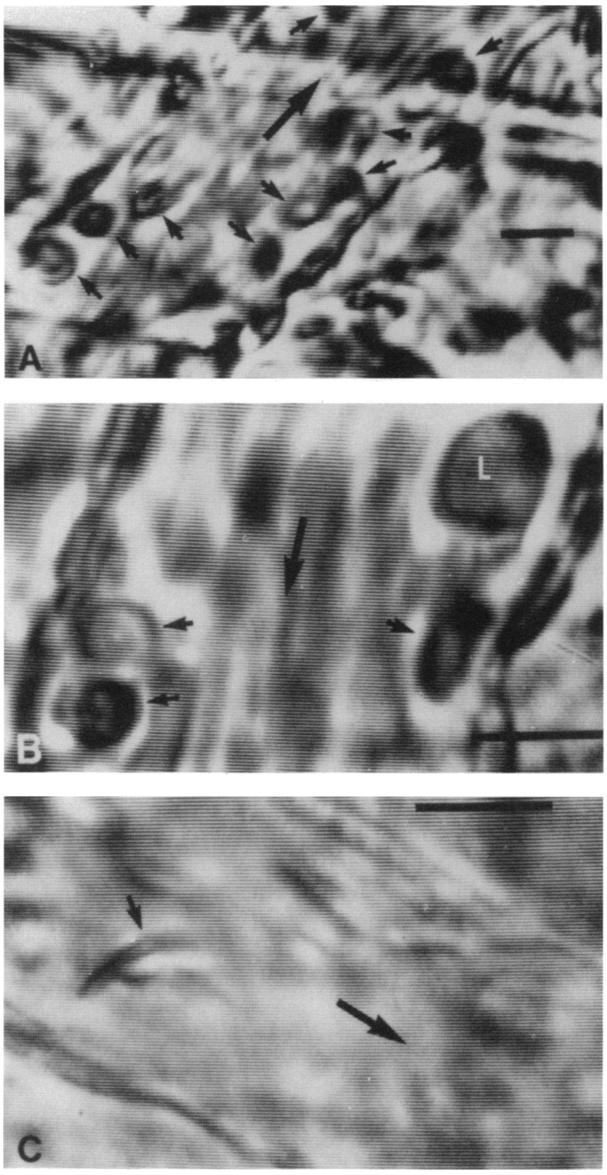

Figure 2. Videomicrograph showing in vivo adherence of red cells to the endothelium of postcapillary venules in the cremaster muscle microvasculature of a $\alpha^{H}\beta^{S}\beta^{S\text{-Antilles}}[\beta^{MDD}]$ mouse. (*A*) Adherent red cells (*small arrows*) during steady state flow (*large arrow*). (*B*) A rolling leukocyte (*L*) is distinguished from adherent red cells (*small arrows*) by its larger diameter. The large arrow indicates flow direction. (*C*) A sickled cell with distinct spicules (*small arrow*) in the venular flow (*large arrow*). Bar in each case = 10 μm.

nated with ease, hence diameter and red cell velocity measurements were made in A2, A3, and A4 arterioles and similar order of venules.

Vessel luminal diameter was measured on-line by image shearing using an image-shearing device (model 907; Instruments for Physiology and Medicine, San Diego, CA). Red cell velocity (Vrbc) was measured along the vessel centerline using the dual-slit photodiode technique of Wayland and Johnson (19). The dual-slit photo detector was placed over the projected image of the vessel and on-line analysis of the optical signals was performed using a cross-correlator as described by Tompkins et al. (20) (Model 102 BF; instruments for Physiology and Medicine). Vrbc measurements were made using a water immersion ×40 objective and ×6.3 eyepiece. The wall shear rates were calculated from the mean Vrbc (Vmean) and vessel diameter. The centerline Vrbc was converted to the mean red cell velocity across the vessel diameter using a conversion factor of 1.6 (Vrbc/Vmean = 1.6) originally described by Baker and Wayland (21). Seki and Lipowsky (22) have confirmed the validity of 1.6 ratio of Vrbc/Vmean for transilluminated vessels of the cremaster tissue. Shear rates along the wall of microvessel of a given internal diameter (D) were calculated using the relationship: Wall shear rate = 8 Vmean/D (23). Estimates of volumetric flow rates (Q) were made from Vmean and the vessel cross-sectional area (π $D^2/4$) as described (20, 24). The practicality of flow estimations has been demonstrated by Lipowsky et al. (24, 25) in studies involving nailfold capillary microcirculation of sickle cell patients, as well as in animals exchange transfused with human sickle blood.

In selected experiments, response of the cremaster arterioles to a transient increase in oxygen tension was evaluated for both control and transgenic mice. In these experiments, cremaster resting conditions were maintained as described above using Ringer's bicarbonate solution equilibrated with N_2 and measurements of the diameter and Vrbc were made. To examine the effect of local, transient hyperoxia, the suffusion was changed to Ringer's bicarbonate solution equilibrated with 21% oxygen in the gas mixture containing 5.6% CO_2 and the balance N_2. Oxy suffusion was applied for 5 min. The suffusion was then switched back to N_2-equilibrated solution. Continuous microcirculatory measurements were made during this maneuver.

Hemodynamic and microcirculatory observations in the ex vivo mesocecum vasculature. Ex vivo perfusion studies were performed in the isolated, acutely denervated, artificially perfused rat mesocecum vasculature according to the method of Baez et al. (26) as modified for the study of erythrocytes (7). Arterial perfusion pressure (Pa) was rendered pulsatile with a peristaltic pump. Venous outflow pressure (Pv) was kept at 3.8 mmHg, and the venous outflow rate (Fv) was monitored with a photoelectric drop counter and expressed as milliliters per minute. During perfusion with Ringer's at Pa of 60 mmHg, a bolus of control or transgenic mouse red cells (hematocrit [Hct] 30% in autologous plasma, 0.2 ml vol) was infused. Peripheral resistance units (PRU) were determined as described (27) and expressed in mmHg/ml per min/gram, PRU = $\Delta P/Q$, where ΔP is the arteriovenous pressure difference and Q is the rate of venous outflow (ml/min) per gram of tissue weight. In each experiment, pressure flow recovery time (Tpf) was determined after the bolus infusion of the samples. Tpf is defined as the time (seconds) required for Pa and Fv to return to their baseline levels after sample delivery and provides an estimate of total transit time through the mesocecum vasculature. These measurements were accompanied by direct intravital microscopic observations and video-recording of the microcirculatory events.

Transmission electron microscopy (TEM). For TEM, tissue samples from the contralateral cremaster muscle were fixed in Karnovsky fixative and processed for TEM as described (28). Sections were stained with uranyl acetate followed by lead citrate and observed in an electron microscope (1200 Ex; JEOL U.S.A. Inc., Peabody, MA) at an accelerating voltage of 80 kV.

Statistical analysis. Paired *t* test or unpaired Student's test was applied to analyze data. The statistical analysis was performed using Statgraphics Plus 5.2 program (STSC, Inc., Rockville, MD) and an IBM-AT computer (IBM Corp., Armonk, NY).

Results

Table I shows hematological parameters in control and $\alpha^{H}\beta^{S}\beta^{S\text{-Antilles}}[\beta^{MDD}]$ mice. $\alpha^{H}\beta^{S}\beta^{S\text{-Antilles}}[\beta^{MDD}]$ mice showed a slight decrease in Hct, which was accompanied by elevated MCHC and percent reticulocytes as compared with controls. The slightly reduced mean corpuscular volume and constant MCH are both consistent with the elevated MCHC.

In the present studies, two categories of experiments were performed: (*a*) Direct in vivo microcirculatory observations involving the cremaster muscle preparation of mice, and (*b*)

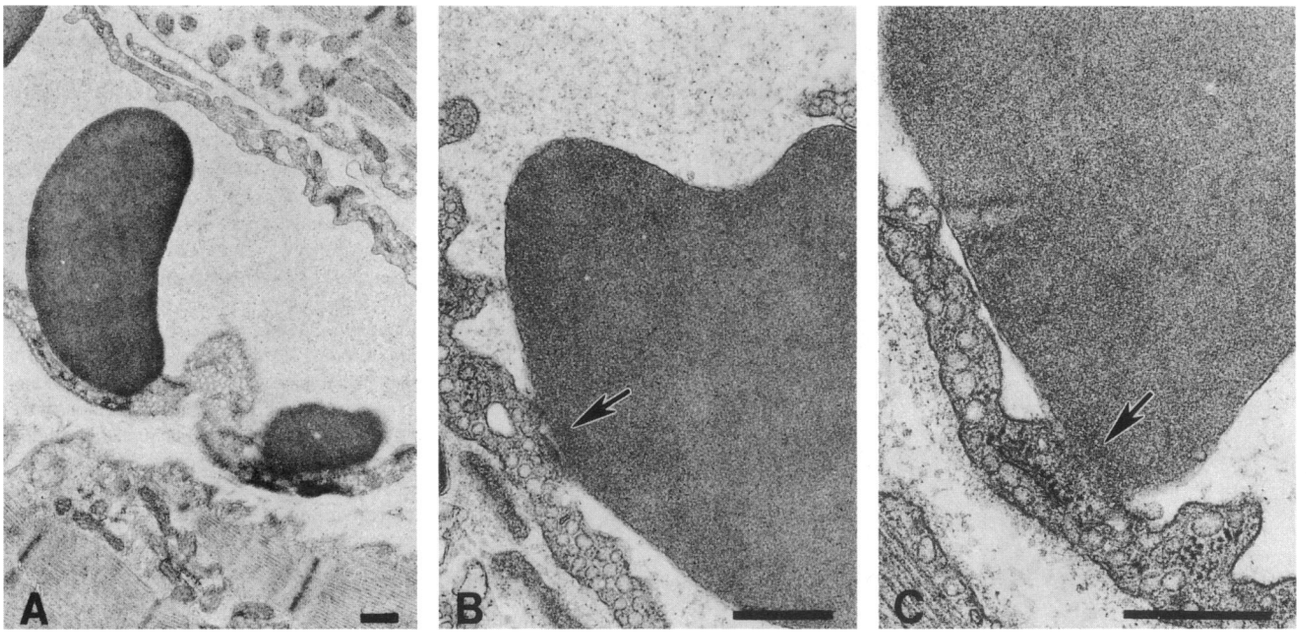

Figure 3. Transmission electron microscopy of the cremaster muscle of $\alpha^{H}\beta^{S}\beta^{S\text{-Antilles}}[\beta^{MDD}]$ showing red cell adhesion to the venular endothelium. (*A*) Adherent red cells in a venule. (*B* and *C*) Higher magnification showing distinct contacts between the red cell membrane and the endothelial surface of venules. Bar in each case = 0.5 μm.

Ex vivo evaluation of hemodynamic and adhesive behavior of $\alpha^{H}\beta^{S}\beta^{S\text{-Antilles}}[\beta^{MDD}]$ mouse red cells.

Direct in vivo microcirculatory observations

In vivo red cell adhesion and circulating sickled cells (intravascular sickling). Direct microscopic observations and videotaping of cremaster microcirculatory flow under resting conditions revealed adhesion of red cells exclusively to the endothelium of postcapillary venules (Fig. 2, *A* and *B*) in 7 out of 9 $\alpha^{H}\beta^{S}\beta^{S\text{-Antilles}}[\beta^{MDD}]$ mice studied, but not in control mice. Increased adhesion of red cells was observed at vessel junctions. In most instances, red cells remained adhered for the duration of experiments. In some venules, both red cells and leukocytes were seen adhering to the vessel wall. Adhering and rolling leukocytes were recognizable by their larger diameters (Fig. 2 *B*). In addition, in transgenic mice showing red cell adhesion, a few sickled cells with distinct spicules (circulating sickled cells) were regularly observed in the venular flow (Fig. 2 *C*). In many instances, transient vessel occlusion, lasting several minutes, was seen at postcapillary level which was spontaneously dislodged by the upstream pressure gradient. In the areas of transient occlusion, a number of red cells appeared distorted and sickled. In addition, in few cases, a permanent occlusion of capillaries and postcapillary venules was observed, characterized by the presence of many morphologically distorted cells.

TEM of the contralateral cremaster muscle, which had not

Table II. Resting Microvascular Diameters (μm) in Control and $\alpha^{H}\beta^{S}\beta^{S\text{-Antilles}}$ [β^{MDD}] Mice

Vessel order	Control mice	$\alpha^{H}\beta^{S}\beta^{S\text{-Antilles}}[\beta^{MDD}]$ mice	*P* value
Arterioles			
A2	45.5±5.9 (13)	44.5±4.5 (10)	0.66
A3	26.0±5.8 (9)	29.7±3.3 (7)	0.15
A4	13.7±4.4 (6)	13.1±2.9 (6)	0.80
Venules			
V2	65.1±13.4 (9)	61.8±11.8 (7)	0.62
V3	34.0±5.5 (8)	34.4±4.9 (6)	0.91
V4	18.9±3.6 (5)	16.9±1.9 (5)	0.27

Values are mean±SD. Numbers in parentheses represent the number of vessels.

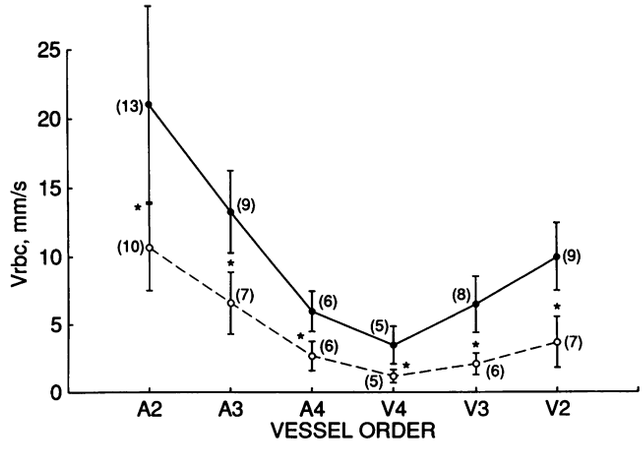

Figure 4. Arteriovenous Vrbc profiles in the resting cremaster muscle microcirculation of controls (● — ●) and $\alpha^{H}\beta^{S}\beta^{S\text{-Antilles}}[\beta^{MDD}]$ (○----○) mice. In general, there was a progressive decrease in red cell velocities with successive branching of arterioles from A2 to A4. Minimum red cell velocity was recorded in V4 venules. However, as compared with controls, the transgenic mice, under resting conditions, showed 50% or more decrease in Vrbc in arterioles. In the venules, the decrease was > 65%. * $P < 0.01$–0.001.

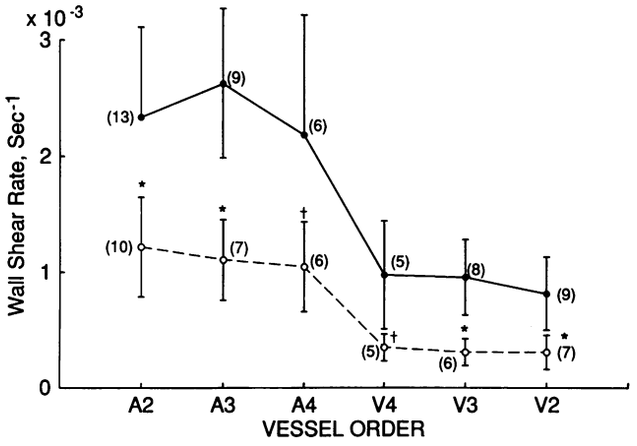

Figure 5. Arteriovenous wall shear rates profiles in the resting cremaster muscle microcirculation of control (• — •) and $\alpha^{H}\beta^{S}\beta^{S\text{-Antilles}}[\beta^{MDD}]$ (○----○) mice. As is evident, during resting conditions, the transgenic mice showed a drastic reduction in wall shear rates in both arterioles and venules. In general, there was almost 50% reduction in arteriolar wall shear rates. Greater than 60% reduction in wall shear rates was observed in V2 vessels. * $P < 0.05$ and $^{+}P < 0.01$–0.001.

been exteriorized, from two $\alpha^{H}\beta^{S}\beta^{S\text{-Antilles}}[\beta^{MDD}]$ mice confirmed adhesion of red cells to the venular endothelium (Fig. 3, *A–C*). The adhered red cells showed distinct contacts between the red cell membrane and the endothelial surface. No adhesion of leukocytes was evident in TEM of the nonexteriorized cremaster, suggesting that adhesion of leukocytes observed above in the cremaster microcirculatory preparation could be a consequence of tissue exteriorization as observed by others (29).

No significant differences were noted in the systemic blood pressure (Psys) of control and the transgenic mice (control, 103.1±7.1 mmHg±SD; transgenic, 104.2±8.7; $P > 0.8$).

Microcirculatory flow measurements under resting conditions. To determine microcirculatory consequences of red cell adhesion and intravascular sickling, on-line recordings of microvascular diameters and centerline red cell velocity (Vrbc) were made under resting conditions (pO_2 of suffusion solution, 15–20 mmHg). From these parameters, wall shear rates and volumetric flow rates (Q) were computed for A2, A3, and A4 arterioles and similar orders of venules. A comparison of the resting microvascular diameters revealed no significant differences between control and $\alpha^{H}\beta^{S}\beta^{S\text{-Antilles}}[\beta^{MDD}]$ mice (Table II). Fig. 4 shows microvascular Vrbc profiles for control and $\alpha^{H}\beta^{S}\beta^{S\text{-Antilles}}[\beta^{MDD}]$ mice. In controls, there was a progressive decrease in Vrbc with successive branching of arterioles from A2 to A4 (Vrbc, mm/s±SD: A2, 21.1±7.1; A3, 13.3±3.0; A4, 6.0±1.5). Minimum Vrbc was recorded in V4 venules, and thereafter a gradual increase in Vrbc was noted in higher orders of venules (V3 and V2) (V4, 3.5±1.4; V3, 6.5±2.1; V2, 10.0±2.5). As compared with controls, $\alpha^{H}\beta^{S}\beta^{S\text{-Antilles}}[\beta^{MDD}]$ mice, under resting conditions, showed a significantly decreased Vrbc in both arterioles and venules. In arterioles, Vrbc showed a decrease of ~ 50% or more (A2, 10.7±3.2; A3, 6.6±2.3; A4, 2.7±1.1; $P < 0.01$–0.001 as compared with controls) (Fig. 4). The decrease in Vrbc was even more pronounced (> 60%) in venules (V4, 1.2±0.5; V3, 2.1±0.8; V4, 3.7±1.9; $P < 0.01$–0.001 as compared with controls).

A plot of arteriovenous wall shear rates (8 Vmean/D) is presented in Fig. 5. In controls, maximum wall shear rates (2,630±640 s^{-1}) were recorded in A3 arterioles (diameter, 29.7±3.3 μm; mean±SD). Thereafter, there was a gradual decline and minimal values were obtained in V2 venules (815±321 s^{-1}). The transgenic mice showed a drastic reduction in wall shear rates (~ 50% or more) in both arterioles and venules ($P < 0.05$ to $P < 0.001$). In the transgenic mice, maximum wall shear rates of 1,221±427 s^{-1} obtained in A2 vessels were ~ 50% less than that recorded for control A2 ($P < 0.001$). Greater than 60% reduction in wall shear rates (e.g., V2 – 312±151) was observed in any given order of venules as compared with controls ($P < 0.02$–0.001) (Fig. 5).

A plot of averaged arteriovenous volumetric flow rates (Q) in the resting microvasculature showed a parabolic pattern in both control and transgenic mice (Fig. 6). In each group, highest flow rates were obtained in A2 and V2 vessels. However, Q (nl/s±SD) was significantly reduced in the transgenic mice (A2 control – 22.0±10.1, A2 transgenic – 10.2±2.9, $P < 0.01$; V2 control – 21.6±10.9, V2 transgenic – 7.2±4.9, $P < 0.01$). The lowest Q values were obtained in V4 postcapillary venules (control – 0.60±0.26, transgenic – 0.18±0.09, $P < 0.01$). Thus transgenic mouse venules showed maximal (~ 70%) decline in Q. The large standard deviations at certain data points in Fig. 6 are mainly due to variations in Vrbc and diameters within a given vessel order.

The effect of oxygen on arteriolar diameter and flow. In selected experiments, involving five controls and three transgenic mice, the effect of a transient increase in local oxygen tension on the arteriolar diameters, Vrbc and estimated volumetric flow rate (Q) was examined (Table III). First, diameters and Vrbc were recorded for control or transgenic mouse arterioles under the resting condition using N_2-equilibrated suffusion solution. Thereafter, the cremaster preparation was suffused for 5 min with solution bubbled with a gas mixture containing 21% oxygen (oxygen tension, 150 mmHg). In the control cremaster, oxygen caused maximal arteriolar vasoconstriction within 3 min. In one out of six control preparations, there was no arteriolar response to oxygen and the preparation was considered non-

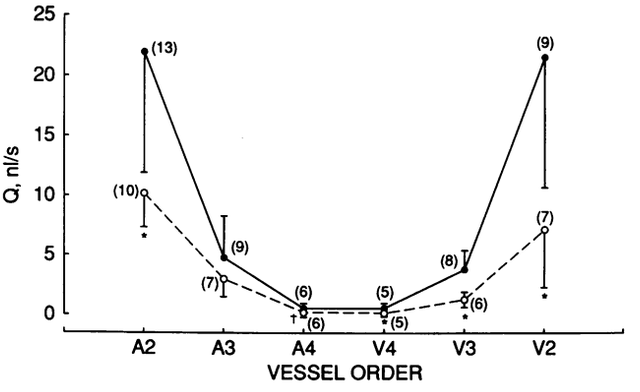

Figure 6. Arteriovenous Q profiles in the resting cremaster muscle microcirculation of control (• — •) and $\alpha^{H}\beta^{S}\beta^{S\text{-Antilles}}[\beta^{MDD}]$ (○----○) mice. Note the parabolic pattern of flow distribution from A2 to V2 vessels. The transgenic mice showed a significant (> 50%) decrease in Q in A2 arterioles. Minimal Q values were estimated for small diameter V4 venules. Also, the transgenic mice showed > 60% decline in venular flow rates. * $P < 0.05$ and $^{+}P < 0.01$.

Table III. Effect of Oxygen (21%) on the Arteriolar Diameter, Vrbc, and Q in the Control and $\alpha^H\beta^S\beta^{S\text{-}Antilles}$ [β^{MDD}] Mice

Mice	Diameter, μm			Vrbc, mm/s			Q, nl/s		
	N_2	O_2	*P* value	N_2	O_2	*P* value	N_2	O_2	*P* value‡
Control	40.1±10.0	12.3±7.2	0.001	18.2±8.0	5.0±4.7	0.001	17.4±15.2	0.9±1.7	0.03
$\beta^S + \beta^{S\text{-}Antilles}$	38.6±8.8	35.1±7.3	0.02	6.5±2.5	10.9±3.8	0.002	5.2±3.2	7.2±4.1	0.03

Values are mean±SD. * In these experiments, five control mice and three transgneic mice were used (number of arterioles [A2 and A3]: control - 6, transgenic - 5). ‡ Paired *t* test.

regulating in accordance with the criteria established before (30), and therefore results include data form five regulating preparations (six arterioles). In the controls, oxygen caused 69.3% decrease in the arteriolar diameter ($P > 0.001$) (Table III and Fig. 7). Concomitant with the diameter decrease, arteriolar Vrbc and Q declined by 74.8% ($P < 0.001$) and 96.5% ($P < 0.03$), respectively (Table III and Fig. 7). In contrast, in $\alpha^H\beta^S\beta^{S\text{-}Antilles}$ [β^{MDD}] mice (five arterioles), the application of oxygenated suffusion solution caused only 8.3% decrease in the diameters ($P > 0.02$) (Table III and Fig. 7); this difference in response was highly significant as compared with controls ($P > 0.0001$; Fig. 7) and indicative of an altered microvascular response. Furthermore, oxygenation caused 68.4% increase in arteriolar Vrbc in the transgenic mice ($P < 0.02$) (Table III); $P > 0.0001$ compared with percent change (−74.8%) in controls (Fig. 7). These changes were accompanied by 41.5% increase in Q ($P < 0.03$) (Table III); $P < 0.0001$ compared with percent change (−96.5%) in control (Fig. 7). This is suggestive of an improved rheologic behavior consequent to absence of sickling of transgenic mouse red cells upon oxygenation. The observed response in the diameter, Vrbc and Q to increase in oxygen tension was almost completely reversible when suffusion was switched back to deoxy Ringer's solution.

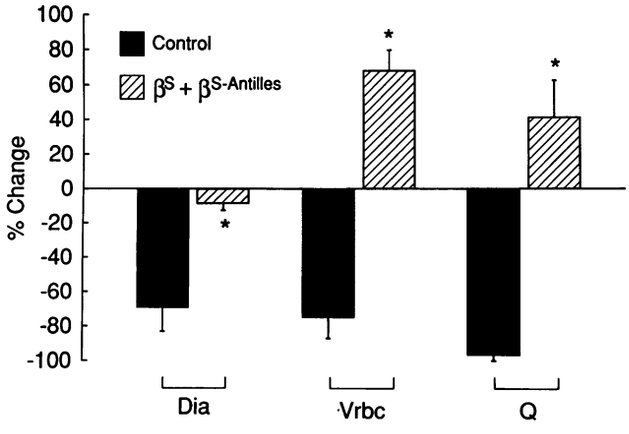

Figure 7. The effect of oxygen (21%) on the arteriolar diameter (*Dia*) Vrbc, and volumetric flow rates (*Q*) in the cremaster muscle microcirculation of control and $\alpha^H\beta^S\beta^{S\text{-}Antilles}$[$\beta^{MDD}$] mice. When oxygen tension of solution suffusing the cremaster was raised to ~ 150 mmHg using 21% oxygen in the gas mixture, the control arterioles showed a pronounced 69.3% decrease in the diameters, accompanied by 74.8% decline in Vrbc. In contrast, under similar conditions, the transgenic mice showed only a slight ~ 8% decrease in diameter, showing an altered microvascular response to oxygen. Also, oxygen caused 68.4% increase in red cell velocity and 41.5% increase in Q, suggesting an improved rheologic behavior of transgenic mouse red cells upon oxygenation. * $P < 0.001$ vs control.

Ex vivo observations

Perfusion experiments were performed, using the ex vivo mesocecum preparation, to investigate hemodynamic and adhesive behavior of oxy red cells from control and $\alpha^H\beta^S\beta^{S\text{-}Antilles}$[$\beta^{MDD}$]. We have previously shown that human sickle cells adhere exclusively in postcapillary venules of the ex vivo mesocecum preparation (8, 9). In the present studies, a bolus of oxy control red cells or the transgenic mouse red cells (0.2 ml, Hct 30% in autologous plasma) was infused into the ex vivo preparations during perfusion with Ringer-albumin solution at an arterial pressure of 60 mmHg. As shown in Table IV, in each preparation, $\alpha^H\beta^S\beta^{S\text{-}Antilles}$[$\beta^{MDD}$] mouse red cells resulted in higher PRU and a delayed Tpf as compared with the control cells, which could be due to the reported presence of dense cells and/or to the presence of adherent cells (16). Direct microscopic observations and videotaping revealed adhesion of transgenic red cells, but not of control cells, which was confined to venules. In some venules, adhered cells tend to form clusters (Fig. 8 *A*) and few small-diameter postcapillary venules appeared completely obstructed (Fig. 8 *B*). However, there was considerable variability in the extent of adhesion and some venular networks were devoid of any adherent cells.

Discussion

The studies presented here demonstrate significant effects of the expression of human α, β^S and $\beta^{S\text{-}Antilles}$ globins (on mouse β-major deletional [β^{MDD}] background) on the microvascular blood flow of the mouse. Direct microscopic observations and videotaping of the cremaster microcirculatory flow revealed ad-

Table IV. Hemodynamic Behavior of $\alpha^H\beta^S\beta^{S\text{-}Antilles}$ [β^{MDD}] Mouse Red Cells in the Ex Vivo Mesocecum Preparation

RBCs	ΔPRU (%)*	Tpf (s)‡
Preparation No. 1		
Control mouse	14.5	75
$\beta^S + \beta^{S\text{-}Antilles}$ mouse	18.5	115
Preparation No. 2		
Control mouse	19.0	45
$\beta^S + \beta^{S\text{-}Antilles}$ mouse	26.4	55

* ΔPRU (%) = PRU RBCs/PRU Ringer's × 100. ‡ Tpf (s) = Pressure-flow recovery time to the baseline level.

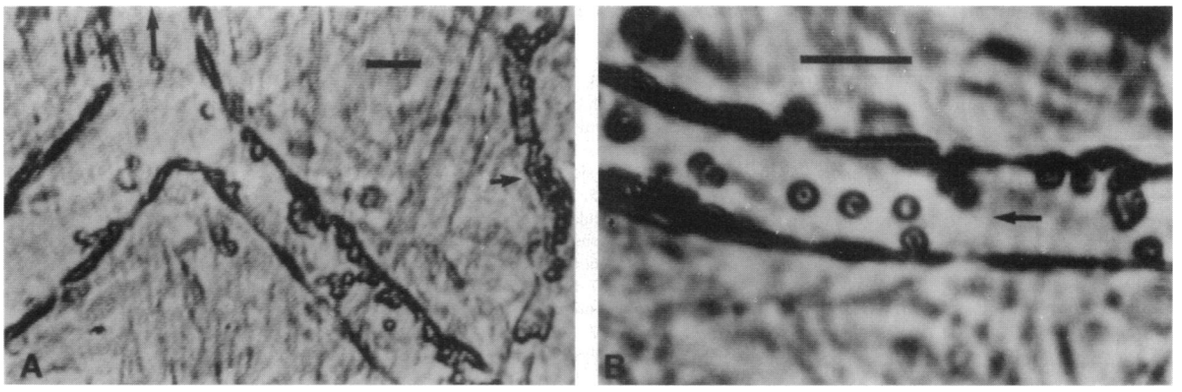

Figure 8. Ex vivo mesocecum microvasculature. Infusion of oxy red cells from $\alpha^{H}\beta^{S}\beta^{S\text{-Antilles}}[\beta^{MDD}]$ was followed by adhesion of these cells exclusively in venules. (*A*) Adhered cells show greater concentration in smaller diameter venules. The arrow indicates the flow direction. (*B*) Adhered mouse cells in a venule are deformed in the direction of the flow (*arrow*). Bar in each case = 20 μm.

hesion of red cells to the vascular endothelium and intravascular sickling under in vivo flow conditions in seven out of nine $\alpha^{H}\beta^{S}\beta^{S\text{-Antilles}}[\beta^{MDD}]$ mice with > 78% combined expression of human β^{S} and $\beta^{S\text{-Antilles}}$. Both red cell adhesion and sickling, considered integral aspects of the pathophysiology of human sickle cell disease, have not been previously demonstrated under in vivo flow conditions.

Adhesion of red cells was restricted to venules in the cremaster muscle preparation of the transgenic mice, as well as in the rat ex vivo mesocecum preparation infused with transgenic red cells. TEM of the nonexteriorized contralateral cremaster muscle of transgenic mice showed distinct contacts between the red cell membrane and the endothelial surface. The venular specificity of adhesion is in agreement with our earlier findings with human SS cells in the ex vivo mesocecum preparation (8, 9), and shows the relevance of the ex vivo preparation in adhesion studies.

In addition, a few sickled cells with distinct spicules were regularly observed in the venular flow of the transgenic mice. Measurements of the delay time of polymerization have shown that ~ 20% $\alpha^{H}\beta^{S}\beta^{S\text{-Antilles}}[\beta^{MDD}]$ mouse red cells would sickle in < 1 s (16). The transgenic mouse red cells showing intravascular sickling are likely to belong to this category.

Since mouse red cells containing human sickle hemoglobin show both sickling and adhesion in vivo, transgenic sickle mice could serve as a useful model for a better understanding of certain in vivo processes involved in the pathophysiology of the human disease.

When the resting microvascular diameters in the cremaster muscle preparation of $\alpha^{H}\beta^{S}\beta^{S\text{-Antilles}}[\beta^{MDD}]$ mice (showing red cell adhesion and sickling) were compared with the control mice, no significant difference was evident, demonstrating no apparent change in the resting vascular tone of transgenic mice. The microvascular profiles of Vrbc, wall shear rates, and Q in the cremaster muscle of control mice are in general agreement with previous studies in different microcirculatory beds of other mammalian species (31). Thus the maximum Vrbc is encountered in A2 arterioles and the minimum in the small diameter V4 venules, before rising again in larger diameter V3 and V2 vessels. Similarity, the highest wall shear rates are recorded on the arteriolar side and lowest on the venular side. However, under the resting conditions, the microvascular Vrbc, wall shear rates and Q showed significant decrease in $\alpha^{H}\beta^{S}\beta^{S\text{-Antilles}}[\beta^{MDD}]$ mice. The impaired microvascular flow in the transgenic mouse under the resting condition (po_2, 15–20 mmHg) is likely a result of intraeythrocytic HbS polymer formation and the observed intravascular sickling. HbS polymerization (hence sickling) results in an increased viscosity and a reduced deformability of red cells (7, 32).

The lower Vrbc in the transgenic mouse, by prolonging arteriovenous transit time of red cells, would further contribute to the observed red cell adhesion and sickling in venules. In fact, venular Vrbc, wall shear rates and Q in the transgenic mice showed greatest decrease (> 60%) as compared with controls. Also, despite reduced Vrbc and wall shear rates in the transgenic mouse arterioles, there was no evidence of red cell adhesion in these vessels, suggesting that adhesion receptors were restricted to the venular endothelium. These observations support our earlier hypothesis that both endothelial characteristics and lower wall shear rates in venules would be required for abnormal adhesion of sickle cells to this part of the microcirculation (9). Thus, the present observations combined with our previous observations on human SS cell adhesion in the ex vivo preparation (8, 9) show that postcapillary venules are likely to be important sites of vasoocclusion. Future work will be required to establish whether, in the transgenic mouse, intravascular sickling generates secondary abnormalities in both the red cell membrane and the vascular endothelium.

Experiments performed to determine the effect of local, transient hyperoxia (using 21% oxygen in the gas mixture) revealed striking differences in the microvascular response of control and transgenic mice. In the controls, the increase in local oxygen tension caused a pronounced 69% decrease in the arteriolar diameter, accompanied by a profound decrease in Vrbc and Q (75 and 96%, respectively). Previous studies with skeletal muscle preparations and isolated rat cremaster muscle arterioles have shown a pronounced vasoconstricting effect of oxygen, while hypoxia results in vasodilation (33–35). Thus microvascular flow and resistance in the skeletal muscle would be significantly modulated by changes in local oxygen tension. Vasoconstriction evoked by increased oxygen tension has been attributed to the inhibition of endothelial synthesis of prostaglandins and is dependent on the presence of intact endothelium (35).

In contrast, in $\alpha^{H}\beta^{S}\beta^{S\text{-Antilles}}[\beta^{MDD}]$ mice, transient hyperoxia resulted in only ~ 8% arteriolar constriction, indicating an altered microvascular response. Also, in transgenic mice,

hyperoxia induced a significant net increase in the arteriolar Vrbc and Q (68 and 41.5%, respectively) (Fig. 7). In view of the observed intravascular sickling during resting conditions, the absence of sickling following the application of oxygen would indicate unsickling of red cells due to depolymerization of HbS and $HbS^{Antilles}$. In general, vasoconstriction results in a decrease in the flow (as seen in control mice) while an increase in the flow is observed after vasodilation (36). In transgenic mice, the net increase in Vrbc and Q during transient hyperoxia, despite a slight vasoconstriction, is likely to be a consequence of unsickling and a decrease in the bulk viscosity. The bulk viscosity of transgenic mouse red cells is significantly higher in the deoxygenated state (data not shown), which is in accordance with our studies on the viscosity behavior of human SS cells (7).

On the other hand, the altered vessel diameter response to oxygen in transgenic mice may be in part a consequence of an increase in the flow. Although the exact mechanism remains to be elucidated, this response could involve either release of specific endothelial molecules (prostaglandins and/or nitric oxide) or vessel diameter compliance secondary to an increased blood flow as suggested for flow-mediated vasodilation in large arteries (37–39). Blood rheological factors have been implicated in the flow intermittency observed in sickle cell patients (40), as well as in a depressed postocclusive reactive hyperemia during the crisis (24). However, there could also be intrinsic differences in the endothelial cell and/or vascular smooth muscle function between controls and transgenic mice. In particular, additional contributions from possible endothelial abnormalities (inflicted by circulating dense cells, adhesion and intravascular sickling) which could induce, for example, increased prostacyclin production (41) cannot be ruled out in the altered vascular tone response to oxygen.

To conclude, the transgenic mice expressing human β^S and $\beta^{S\text{-}Antilles}$ on the mouse β-major deletional background exhibit red cell endothelial interaction and intravascular sickling, both of which have been implicated in the pathophysiology of the human sickle cell disease, but never been demonstrated before in vivo under dynamic flow conditions. In addition, we find a novel phenomenon, an altered microvascular tone, and flow response to oxygen in the transgenic mice. One implication of this finding is that if an incompletely obstructed vessel could be reached to provide adequate level of oxygenation, some of the vasoocclusion could be averted. Taken as a whole, the microvascular flow abnormalities would contribute to the observed organ damage and a reduced life span in these transgenic mice. Finally, the transgenic mouse models present a unique opportunity for further investigations of vasoocclusive mechanisms and to test potential therapies in vivo.

Acknowledgments

We would like to thank Xiao-du Liu and Sandra Suzuka for their excellent technical assistance.

This work was supported by National Institutes of Health grants HL-45931, HL-37212, and AI 34064, and by the American Heart Association (New York Affiliate).

References

1. Kaul, D. K., and R. L. Nagel. 1993. Sickle cell vasoocclusion: many issues and some answers. (*Basel*). 49:5–15.

2. Hebbel, R. P., O. Yamada, C. F. Moldow, H. S. Jacob, J. G. White, and J. W. Eaton. 1981. Abnormal adherence of sickle erythrocytes to cultures vascular endothelium: possible mechanism for microvascular occlusion in sickle cell disease. *J. Clin. Invest.* 65:154–160.

3. Hebbel, R. P., C. F. Moldow, and M. H. Steinberg. 1981. Modulation of erythrocyte-endothelial interactions and the vasoocclusive severity of sickling disorders. *Blood.* 58:947–952.

4. Hoover, R., R. Rubin, G. Wise, and R. Warren. 1985. Adhesion of normal and sickle erythrocytes to endothelial monolayers. *Blood.* 54:872–876.

5. Mohandas, N., and E. Evans. 1985. Sickle erythrocyte adherence to the vascular endothelium: morphological correlates and the requirement for divalent cations and collagen-binding plasma proteins. *J. Clin. Invest.* 76:1605–1612.

6. Barabino, G. A., L. V. McIntire, S. G. Eskin, D. A. Sears, and M. Udden. 1987. Endothelial interactions with sickle cells, sickle trait, mechanically injured, and normal erythrocytes under controlled flow. *Blood.* 70:152–157.

7. Kaul, D. K., M. E. Fabry, P. Windisch, S. Baez, and R. L. Nagel. 1983. Erythrocytes in sickle cell anemia are heterogeneous in their rheological and hemodynamic properties. *J. Clin. Invest.* 72:22–31.

8. Kaul, D. K., M. E. Fabry, and R. L. Nagel. 1989. Microvascular sites and characteristics of sickle cell adhesion to vascular endothelium in shear flow conditions: pathophysiological implications. *Proc. Natl. Acad. Sci. USA.* 86:3356–3360.

9. Kaul, D. K., D. Chen, and J. Zhan. 1994. Adhesion of sickle cells to vascular endothelium is critically dependent on changes in density and shape of the cells. *Blood.* 83:3006–3017.

10. Greaves, D. R., P. Fraser, M. A. Vidal, M. A. Hedges, D. Ropers, L. Luzzatto, and F. Grosveld. 1990. A transgenic mouse model of sickle cell disorder. *Nature (Lond.).* 343:183–185.

11. Ryan, T. M., T. M. Townes, M. P. Reilly, T. Asakura, R. P. Palmiter, and R. R. Behringer. 1990. Human sickle hemoglobin in transgenic mice. *Science (Wash. DC).* 247:566–568.

12. Rubin, E. M., H. E. Witkowska, E. Spangler, P. Curtin, N. Mohandas, and B. H. Lubin. 1991. Hypoxia-induced in vivo sickling of transgenic mouse red cells. *J. Clin. Invest.* 87:639–647.

13. Trudel, M., M. E. De Paepe, N. Chretien, S. Nacera, J. Jacmain, M. Sorette, T. Hoang, and Y. Beuzard. 1994. Sickle cell disease of transgenic SAD mice. *Blood.* 84:3189–3197.

14. Fabry, M. E., R. L. Nagel, A. Pachnis, S. M. Suzuka, and F. Costantini. 1992. High expression of human β^S- and α-globin chains in transgenic mice: hemoglobin composition and hematological consequences. *Proc. Natl. Acad. Sci. USA.* 89:12150–12154.

15. Fabry, M. E., F. Costantini, A. Pachnis, S. M. Suzuka, N. Bank, H. S. Aynedjian, S. M. Factor, and R. L. Nagel. 1992. High expression of human β^S- and α-globin chains in transgenic mice: erythrocyte abnormalities, organ damage, and the effect of hypoxia. *Proc. Natl. Acad. Sci. USA.* 89:12155–12159.

16. Fabry, M. E., A. Sengupta, S. M. Suzuka, F. Costantini, E. M. Rubin, J. Hoftrichter, G. Christoph, E. Mancie, D. Culberson, S. M. Factor, and R. L. Nagel. A second generation of transgenic mouse model expressing HbS and HbS-Antilles results in increased phenotypic severity. *Blood.* 86:2419–2428.

17. Baez, S. 1973. An open cremaster muscle preparation for the study of blood vessels by in vivo microscopy. *Microvasc. Res.* 5:384–394.

18. Chen, D., and D. K. Kaul. 1994. Rheological and hemodynamic characteristics of red cells of mouse, rat and human. *Biorheology.* 31:103–113.

19. Wayland, H., and P. Johnson. 1967. Erythrocyte velocity measurements in microvessels by a two-slit method. *J. Appl. Physiol.* 22:333–337.

20. Tompkins, W., R. R. Monti, and M. Intaglietta. 1974. Velocity measurements by self-tracking correlator. *Rev. Sci. Instrum.* 45:647–649.

21. Baker, M., and H. Wayland. 1974. On-line volume flow rate and velocity profile measurement for blood in microvessels. *Microvasc. Res.* 7:131–143.

22. Seki, J., and H. H. Lipowsky. 1987. In vivo and in vitro measurements of red cell velocity under epifluorescent microscopy. *Microvasc. Res.* 38:110–124.

23. Lipowsky, H. H., S. Usami, and S. Chien. 1980. In vivo measurements of "apparent viscosity" and microvessel hematocrit in the mesentery of the cat. *Microvasc. Res.* 19:297–319.

24. Lipowsky, H. H., N. U. Sheikh, and D. M. Katz. 1987. Intravital microscopy of capillary hemodynamics in sickle cell disease. *J. Clin. Invest.* 80:117–127.

25. Lipowsky, H. H., S. Usami, and S. Chien. 1982. Human SS red cell rheological behavior in the microcirculation of cremaster muscle. *Blood Cells (Berl.).* 8:113–126.

26. Baez, S., H. Lamport, and A. Baez. 1960. Pressure effects in living microscopic vessels. *In* Flow Properties of Blood and Other Biological Systems. A. L. Copley and G. Stainsby, editors. Pergamon Press, London. 122–136.

27. Green, H. D., C. E. Rapela, and M. D. Conard. 1963. Resistance (conductance) and capicitance phenomena in terminal vascular beds. *In* Handbook of Physiology, Section 2 Circulation, Vol. II. W. F. Hamilton and P. Dow, editors. American Physiological Society, Bethesda, MD. 935–960.

28. Kaul, D. K., R. L. Nagel, J. F. Llena, and H. L. Shear. 1994. Cerebral malaria in mice: demonstration of cytoadherence of infected red cells and micror-

heologic correlates. *Am. J. Trop. Med. Hyg.* 50:512–521.

29. Fiebig, E., K. Ley, and K. E. Arfors. 1991. Rapid leukocyte accumulation by "spontaneous" rolling and adhesion in the exteriorized rabbit mesentery. *Int. J. Microcirc. Clin. Exp.* 10:127–144.

30. Prewitt, R. L., and P. C. Johnson. 1976. The effect of oxygen on arteriolar red cell velocity and capillary density in the rat cremaster muscle. *Microvasc. Res.* 12:59–70.

31. Zweifach, B. W., and H. H. Lipowsky. 1984. Pressure-flow relations in blood and lymph microcirculation. *In* Handbook of Physiology, Section 2: Cardiovascular System, Vol. IV, Microcirculation (Part I). E. M. Renkin and C. C. Michen, editors. American Physiological Society, Bethesda, MD. 251–308.

32. Nash, G. B., C. S. Johnson, and H. J. Meiselman. 1986. Influence of oxygen tension on the viscoelastic behavior of red blood cells in sickle cell disease. *Blood.* 67:110–118.

33. Duling, B. R. 1972. Microvascular responses to alterations in oxygen tension. *Circ. Res.* 31:481–489.

34. Hutchins, P. M., R. F. Bond, and H. D. 1974. Participation of oxygen in the local control of skeletal muscle microvasculature. *Circ. Res.* 34:85–93.

35. Messina, E. J., D. Sun, A. Koller, M. S. Wolin, and G. Kaley. 1994. Increases in oxygen tension evoke arteriolar constriction by inhibiting endothelial prostaglandin synthesis. *Microvasc. Res.* 48:151–160.

36. Ballard, S. T., M. A. Hill, and C. A. Meininger. 1991. Effect of vasodilation and vasoconstriction on microvascular pressures in skeletal muscle. *Microcirc. Endothelium Lymphatics.* 7:109–131.

37. Bevan, J. A., E. H. Joyce, and G. C. Wellman. 1988. Flow-dependent vasodilation in a resistance artery still occurs after endothelial removal. *Circ. Res.* 63:980–985.

38. Cooke, J. P., J. Stamler, N. Andon, P. F. Davies, G. McKinely, J. and Loscalzo. 1990. Flow stimulates endothelial cells to release a nitrovasodilator that is potentiated by reduced thiol. *Am. J. Physiol. 259 (Heart Circ. Physiol. 28)*:H804–H812.

39. Fujii, K., D. D. Heistad, and F. M. Faraci. 1991. Flow-mediated dilation of the basilar artery in vivo. *Circ. Res.* 69:697–705.

40. Rodgers, G. P., A. N. Schechter, C. T. Noguchi, H. G. Klein, A. W. Neinhuis, and R. F. Bonner. 1984. Periodic microcirculatory flow in patients with sickle-cell disease. *N. Engl. J. Med.* 311:1534–1538.

41. Chappey, O., M. P. Wautier-Pepin, and J. L. Wautier. 1994. Adhesion of erythrocytes to endothelium in pathological situations: a review article. *Nouv. Rev. Fr. Hematol.* 36:281–288.